Journal of Alloys and Compounds 509 (2011) 6973–6979

Contents lists available at ScienceDirect

Journal of Alloys and Compounds

journal homepage: www.elsevier.com/locate/jallcom

High dielectric constant of $(Ba_{0.96}Ca_{0.04})(Ti_{0.85}Zr_{0.15})O_3$ multilayer ceramic capacitors with Cu doped Ni electrodes

Ying-Chieh Lee [a,*], Chen-Su Chiang [b]

[a] Department of Material Engineering, National Pingtung University of Science & Technology, Pingtung, Taiwan
[b] Department of Electrical Engineering, National Cheng Kung University, Tainan, Taiwan

ARTICLE INFO

Article history:
Received 14 January 2011
Received in revised form 30 March 2011
Accepted 1 April 2011
Available online 9 April 2011

Keywords:
Cu doped Ni electrode
MLCC
Reducing atmosphere
$(Ba_{0.96}Ca_{0.04})(Ti_{0.85}Zr_{0.15})O_3$

ABSTRACT

A nickel paste with Cu dopant was used as the internal electrodes in multi-layer ceramic capacitors (MLCCs) using barium titanate $(Ba_{0.96}Ca_{0.04})(Ti_{0.85}Zr_{0.15})O_3$ ceramic (BCTZ) with copper endtermination. The sintering behaviors of the MLCC and the interfacial structure between the Ni/Cu electrodes and the BCTZ dielectrics have been investigated. The thermal shrinkage and sheet resistance of the Ni/Cu alloys sintered at 1220 °C for 2 h in a reducing atmosphere were measured using thermal analysis techniques (TMA) and four-point probe equipment. The composition distributions, microstructures and line defects were examined using microstructural analysis techniques (SEM/HRTEM) coupled with energy-dispersive spectroscopy (EDS). The Cu alloyed with Ni significantly improves the continuity of the electrode in the MLCC; this is due to there being no mutual trigger reaction between Ni and BCTZ dielectrics. In terms of the electrical properties, the results showed that Ni paste with Cu dopant improves the dielectric constant of the MLCC, but the dielectric loss ($\tan\delta$) is a slightly when higher compared to standard MLCC.

1. Introduction

To keep pace up with the trend in the miniaturization of electronic components, concentrated efforts have been put in forced on the development of small multilayer ceramic capacitors to meet the rapid development of integrated circuit and surface mounting technology. The demand of the multilayer ceramic capacitors in high quality has quickly increased in the past decade [1]. However, the high sintering temperature of BaTiO3 suggested the adoption of high melting point internal electrodes, such as Pd and Ag–Pd alloy. To confront the requirements on smaller size, higher performance and lower cost, the manufacturing techniques of the MLCCs have closely engaged the development of base metal electrode (BME) and thinner dielectric ceramic layers [2–6]. Barium titanate ($BaTiO_3$) is a perovskite structure and has been widely investigated because of its dielectric and ferroelectric properties [7,8]. (Ba, Ca)(Ti, Zr)O_3 ceramics are commonly applied as key materials for high capacitance MLCCs with an application specification of Y5V due to their high dielectric constant. They exhibit broad dielectric maxima (ε_{max}), with peak values of up to $\varepsilon_{max} \approx 18{,}000$ when prepared in oxidizing atmospheres [9]. Ca and Zr are employed in order to broaden the dielectric maximum at the Curie point and shift it to room temperature, respectively. The current trend in the MLCC industry is to manufacture thinner dielectrics thickness (<1.0 μm), so that higher capacitance can be achieved in smaller a size. When the dielectric thickness was reduced <1.0 μm, one of the main problems that arise in thin layer base metal electrode multilayer ceramic capacitors (BME-MLCCs) is the discontinuity of Ni internal electrodes. Consequently, major electrical performances of the capacitors will be strongly affected by this type of structural imperfection and the scaling down of the co-fired MLCC size will be limited. Yang et al. [10] reported that the main acceleration factor for Ni electrodes discontinuity is the formation of a thin liquid alloy layer at Ni–$BaTiO_3$ interfaces during multilayers co-sintering. In order to solve this problem, a thermodynamic approach based on a surface modification of Ni particles with noble metals aimed to prevention the formation of interfacial alloy layer. Cu is selected as the second 3 metallic additives providing a potential alloying phase to Ni [11]. The crystalline structures of copper and nickel are face-centered cubic. However, Cu has an atomic radius just a few percent different to that of Ni. Thermodynamically, the interfacial energy of the Ni alloy system will be different to that of pure Ni. Cu has a high electrical and thermal conductance, and Ni displays high corrosion resistance. For these reasons, a mixture of Ni and Cu was proposed for use as the MLCC electrodes [12,13]. In this paper, the effects of Cu doped Ni electrodes on the sintering behavior, the dielectric properties and the microstructure of BCTZ MLCC are investigated. Moreover, the interfacial reaction between BCTZ and metallic electrodes was studied.

* Corresponding author. Tel.: +886 8 7703202; fax: +886 8 7740552.
E-mail address: YCLee@mail.npust.edu.tw (Y.-C. Lee).

0925-8388/$ – see front matter © 2011 Elsevier B.V. All rights reserved.
doi:10.1016/j.jallcom.2011.04.024

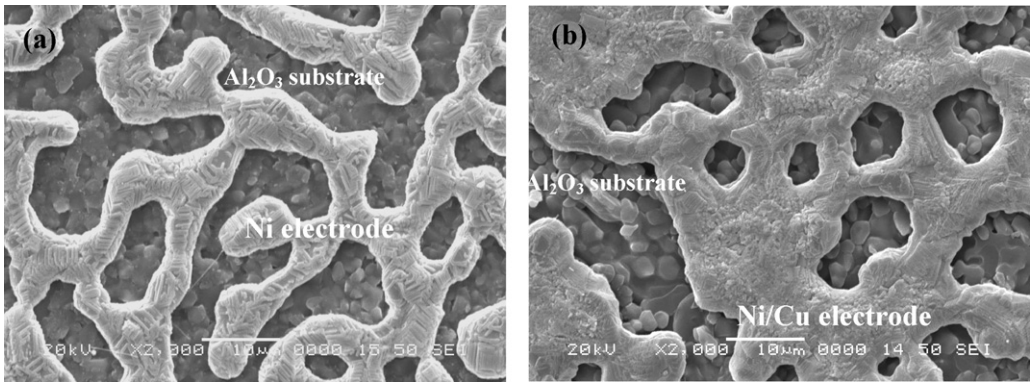

Fig. 1. Scanning electron microscopic micrographs of the Ni paste printed on Al_2O_3 substrate and sintered at 1220 °C with different amounts of (a) 0 mol% and (b) 0.92 mol% Cu addition.

2. Experimental procedure

2.1. Preparation of the BCTZ powders

Conventional ceramic fabrication processes were used to prepare the $(Ba_{0.96}Ca_{0.04})(Ti_{0.85}Zr_{0.15})O_3$ (BCTZ) samples using commercial powders of $BaCO_3$, $CaCO_3$, ZrO_2 and TiO_2. The BCTZ samples were doped with 0.03 mol% Mn acceptor and 0.15 mol% SiO_2 sintering aid in this study. The $BaCO_3$, $CaCO_3$, ZrO_2, TiO_2, MnO_2 and SiO_2 powders were mixed with deionized water for 24 h in a Ø2 mm zirconia ball-mill. The mixture was dried, calcined at 1150 °C for 6 h in air, and then crushed into powder.

2.2. Nickel paste preparation

Cu doped Ni pastes were prepared with different copper addition (e.g. 0.92, 1.84, 2.76, 4.6 and 9.2 mol% copper content). Copper powder was made by Fukuda Co., Ltd. Japan and particle size was about 0.5 μm. The paste properties consist of 50% solid content and 50 Pa s of viscosity by 10 rpm. The paste was rolled several times by a three-roll mill. To measure the shrinkage rate and electrical resistivity of Cu doped Ni paste after sintering, these Cu doped Ni paste were printed on the Al_2O_3 substrate, as well as they were sintered at 1220 °C for 2 h in a reduction atmosphere (in 4 an oxygen partial pressure $<10^{-10}$ Pa). The electrical resistivity of samples was determined by the four-point probe technique.

2.3. Fabrication of multilayered BCTZ capacitors

The BCTZ powders were mixed with resin (polyvinyl butyral), plasticizer (butyl benzyl phthalate) and solvent (toluene and ethanol). The resultant slurry was tape-casted to a green sheet with a 30 μm thickness using the Doctor-blade method. Cu doped Ni paste was printed as an internal electrode onto the green sheet. These printed sheets were stacked, pressed at 60 °C under a pressure of 5.2×10^7 Pa and cut into chips. The laminated green chip was sintered at 1220 °C for 2 h in a reduction atmosphere (in an oxygen partial pressure $<10^{-10}$ Pa) after binder burn out (320 °C), and the sintered chip is called brick. Subsequently, annealing in an oxygen partial pressure below 1.7×10^{-6} Pa at 1000 °C was carried out to reoxidize the ceramic bodies.

2.4. Analysis and measurement

The density of the sintered composites was measured using the Archimedes method. The microstructures of polished samples were examined by scanning electron microscopy (SEM, model S2500, Hitachi, Tokyo, Japan). The mean grain size was calculated using the line intercept method. Copper electrodes were attached to the sintered brick and fired at 900 °C for 10 min to measure its electrical properties. The dielectric permittivity and the dissipation factor of the MLCCs were measured using an impedance analyzer (Agilent Technology HP4284A). The measurement was carried out over temperature range of −30 °C to 85 °C at 1 V rms. The insulation resistance (IR) was measured using a high resistance meter (Agilent Technology HP4339B) at temperature ranging from 25 to 180 °C. The life of insulation resistance was tested in a highly accelerated life test (HALT) in which the acceleration was done by temperature 105 °C and voltage stresses 200 V. The IR lifetime was determined as the time needed to fall to the 10^6 Ω level. Microstructures of samples were investigated by filed-emission transmission electron microscopy (FE-TEM, FEI E.O. Tecnai 5 F20) at an acceleration voltage of 200 kV, equipped with energy-dispersive spectroscopy (EDS).

3. Results and discussion

3.1. Characteristic evaluation for Cu doped Ni thick films

Fig. 1 shows the SEM images of Ni pastes sintered at 1220 °C with Cu concentrations: 0 and 0.92 mol%. High levels of shrinkage were observed for the samples without Cu, as shown in Fig. 1(a). When Cu was doped in Ni paste, the shrinkage of Ni thick films were decreased obviously. The addition of Cu retards the shrinkage of the Ni thick films, leading to better interfacial matching between the Ni film and the Al_2O_3 substrate. Fig. 2 shows the resistivity of the Ni pastes sintered at 1220 °C for various Cu concentrations: 0, 0.92, 1.84, 2.76, 4.6 and 9.2 mol%. It is found that resistivity was significantly decreased with the addition of Cu. The resistivities of the thick films were 3×10^{-2}, 5×10^{-4}, 6×10^{-4}, 5.5×10^{-4}, 6×10^{-4} and 7×10^{-4} Ω cm for 0, 0.92, 1.84, 2.76, 4.6 and 9.2 mol% Cu dopant, respectively. The reason the pure nickel film had a higher resistivity was due to high shrinkage after sintering, as shown in Fig. 1. It is known that the degree of densification is important in determining the electrical behavior of thick films, and the bulk resistivity of the $Ni_{0.7}Cu_{0.3}$ thick film was 7.3×10^{-4} Ω cm [14–16].

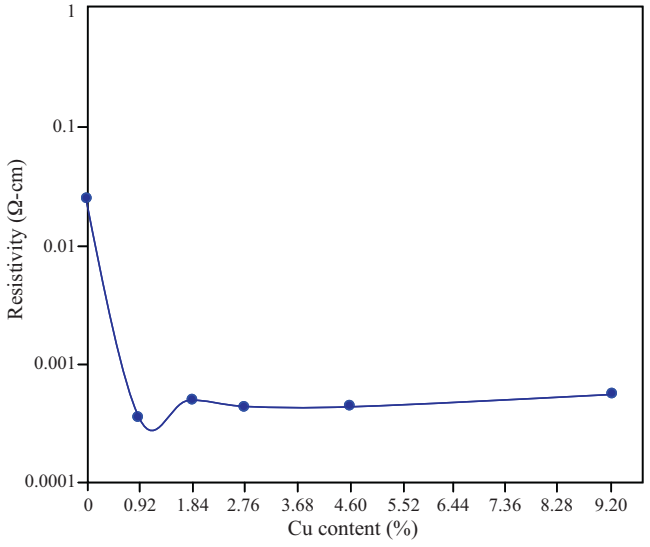

Fig. 2. The electrical resistivity of Ni paste sintered at 1220 °C as a function of the amount of added Cu.

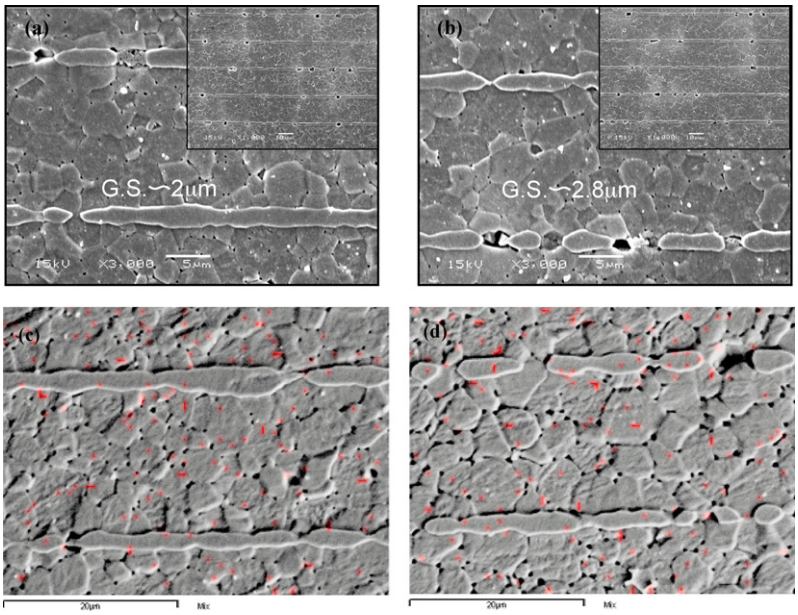

Fig. 3. Microstructure micrographs of the BCTZ MLCCs with (a) SEM: 0.92 mol% Cu, (b) SEM: 2.76 mol% Cu, and Cu elemental mapping with (c) EDS: 0.92 mol% Cu, (d) EDS: 2.76 mol% Cu.

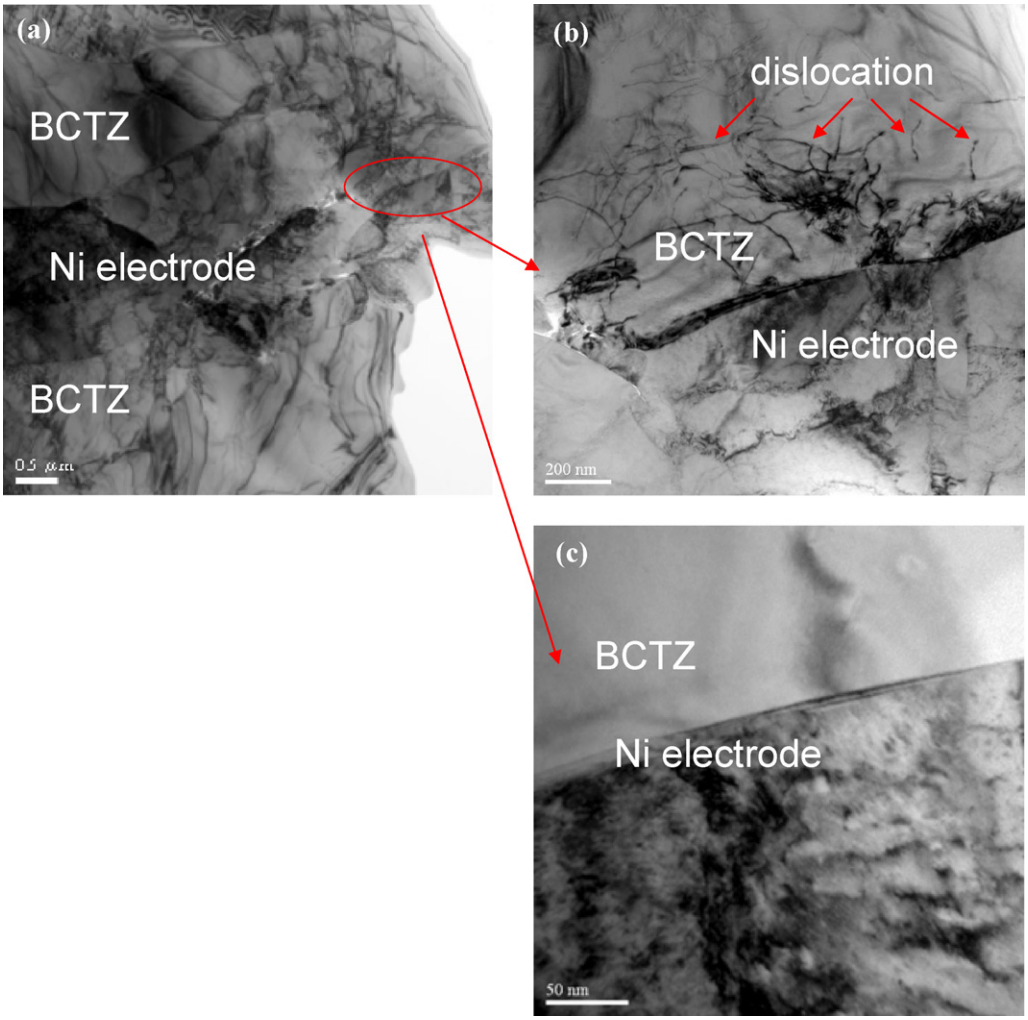

Fig. 4. HRTEM micrographs of the BCTZ MLCC sintered at 1220 °C with a 2.76 mol% Cu doped Ni electrode showing; (a) BCTZ dielectric and metal electrode, (b) dislocations and (c) interface between BCTZ dielectric and metal electrode.

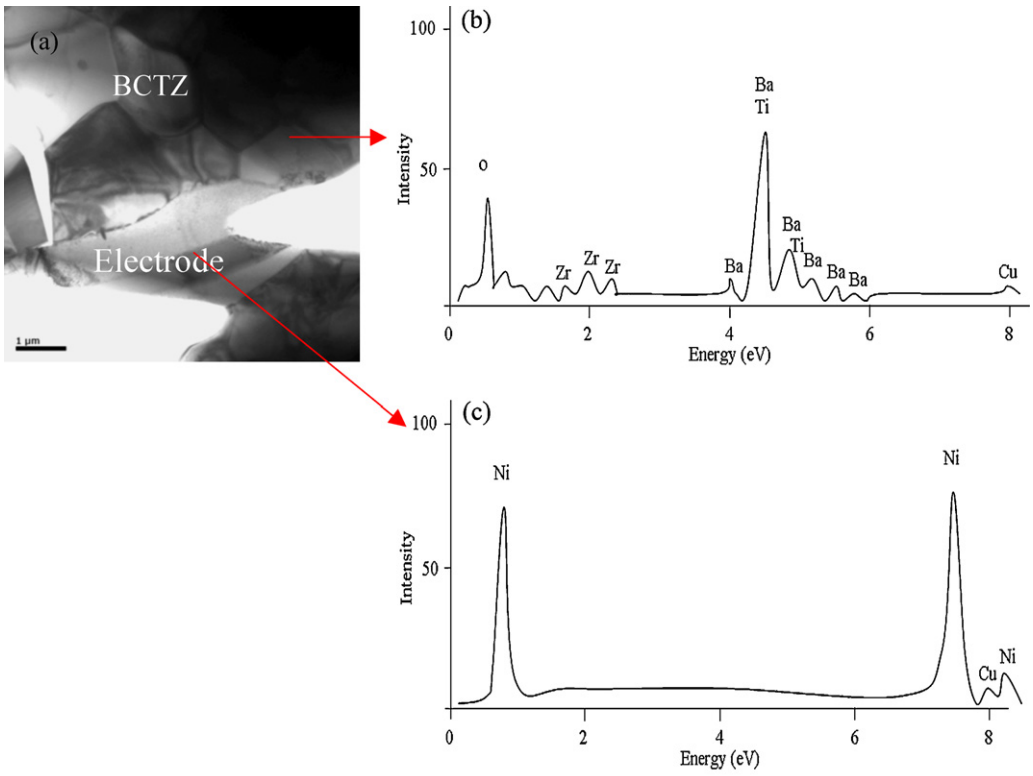

Fig. 5. TEM microstructure of the BCTZ ceramic with 2.76 mol% Cu doped Ni electrodes sintered at 1220 °C for 2 h, showing; (a) morphology, (b) EDS of BCTZ ceramic and (c) EDS of the metal electrode.

3.2. *Effect of Cu doped Ni electrodes on the microstructures of BCTZ MLCC*

A green sheet was prepared by tape casting using the BCTZ powders. Cu doped Ni paste was attached to the green sheet as an internal electrode. After lamination, the green chips were sintered at 1220 °C for 2 h and the external Cu electrodes were designed to be terminating. In order to understand the continuity of the Cu doped Ni paste and microstructures of the dielectrics in the MLCC, a cross-sectional of the MLCC was prepared as shown in Fig. 3. From Fig. 3(a and b), it can be seen that the continuity of the internal electrodes in the MLCC was about 88% with a lay down of approximately 0.6 mg/cm^2. The dielectric film thickness after sintering was approximately 17 μm and the electrode thickness was approximately 2.0 μm. However, the continuity of internal 6 electrodes in commercial MLCCs is below 80% in general with particular reference to the Y5V-1206 MLCCs rated 1 μF and manufactured by Yageo Co. [17]. Pure $BaTiO_3$ powders are often added to the metal electrode so as to decrease the coefficient mismatch of thermal expansion and increase the sintering match with the dielectric layers. Most importantly, interfacial reactions may occur between the internal Cu doped Ni electrode and the dielectric ceramic layer. Fig. 3 also shows the microstructure of a BCTZ MLCC. There is a good physical match between Cu doped Ni electrodes and BCTZ dielectrics resulting from inferior interfacial bonding. To investigate the diffusion of Cu into the dielectric layer after co-firing, Cu elemental mapping was carried out for the MLCCs specimens with 0.92 mol% and 2.76 mol% Cu doped Ni inner electrode as shown in Fig. 3(c and d), respectively. The Cu signal is represented by the red points, thus it was found that the Cu^{2+} diffuses into the BCTZ dielectric layer significantly. It is well known that CuO is incorporated into the BT structure at CuO ~0.6 mol% because of its small ionic radius it can substitute for Ti^{4+}, which is in agreement with the literature [18,19]. The grain size differs between the 0.92 mol% and 2.76 mol% Cu doped Ni MLCC inner electrodes. The grain size for MLCC with 0.92 mol% and 2.76 mol% Cu doped Ni inner electrode was 2.0 μm and 2.8 μm, respectively. This result indicates that more Cu dopant in the Ni electrode leads to grain growth of the BCTZ dielectrics. This may be attributed to the ionic radius of Cu^{2+} (0.73 Å), which is larger than that of Ti^{4+} (0.605 Å) [20]. When Cu substitutes into Ti sites in the perovskite ABO_3 structure, it will create lattice strain and oxygen vacancies. In an ideal cubic perovskite ABO_3 structure, the coordination numbers of the A- and B-sites are 12 and 6, respectively, $t = 0.77–1.1$. The ionic radii of Ba, Ti, O, and Cu are summarized as follows: A-site (12 coordinate): Ba^{2+} = 1.61 Å, B-site (6 coordinate): Cu^{2+} = 0.73 Å, Ti^{4+} = 0.605 Å; O^{2-} = 1.40 Å [21]. Accordingly, the Cu^{2+} would occupy the B sites of the perovskite structure since Cu^{2+} is too small for the A-site. When Cu^{2+} substitutes into the B-site, a doubly ionized oxygen vacancy is formed simultaneously, i.e.

$$CuO \rightarrow Cu''_{Ti} + V''_O + O_O \quad (1)$$

the oxygen vacancy defect reaction will be dominant in $BaTiO_3$. The reaction can be expressed with Kroger–Vink notation [22]:

$$O^x_O \rightleftarrows 1/2O_2(g) + V''_O + 2e^- \quad (2)$$

Further study of the microstructure using high-resolution transmission electron microscopy (HRTEM) was used to clarify the issue and will be discussed later. A HRTEM image of a typical Ni-BCTZ interface obtained from 2.76 mol% Cu doped Ni inner electrode MLCC is shown in Fig. 4. The sample shows the presence of many dislocations in the interface, which is between BCTZ and the metal electrode, as can be seen in Fig. 4(b). This phenomenon can be explained by lattice distortion, which comes about as Cu substitutes for Ti, creating lattice strain and oxygen vacancies. Dislocations are created in the lattice during the solidification of crystalline solids. They are also formed by the permanent or plastic deformation of crystalline solids, vacancy condensation and atomic mismatch in

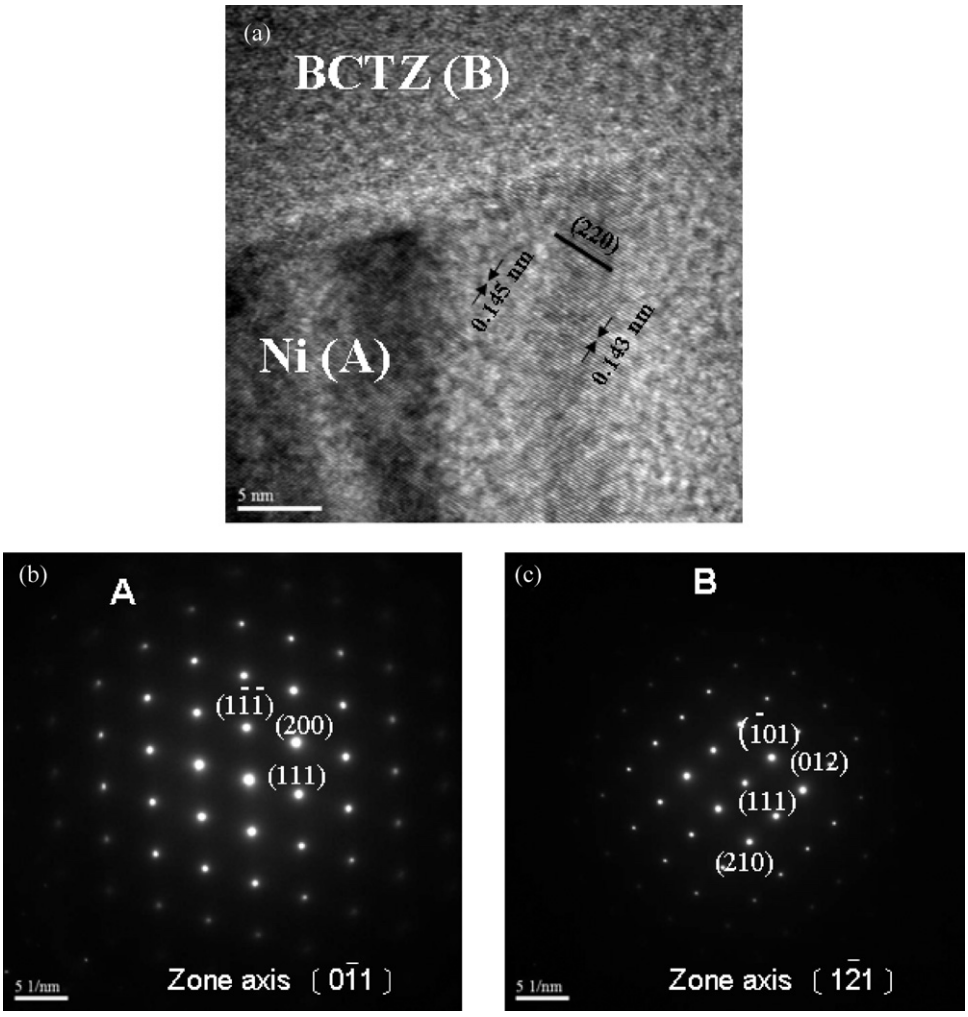

Fig. 6. HRTEM micrographs and selected-area diffraction patterns of a grain in BCTZ MLCC with Cu doped Ni electrodes sintered at 1220 °C (a) TEM micrographs, (b) SAD of BCTZ ceramic and (c) SAD of Cu doped Ni electrode.

solid solutions [23]. Conversely, the intermetallic layers in interface between BCTZ and the metal electrode were not observed, as shown in Fig. 4(c). This means that the interface between BCTZ and the metal electrode is very clear. Yang et al. [10] reported that such observations of the Ni–$BaTiO_3$ interface were performed on more than 20 commercial Ni–$BaTiO_3$ MLCCs supplied by a number of manufacturers. A discrete interface layer was present in all samples. The thickness of the interface layer ranged from 4 to 15 nm, most likely depending on exact doping chemistries, binder chemistries in the Ni electrodes, $BaTiO_3$ powder sources, $BaTiO_3$ tapes, and process histories of different manufacturers. The 2.76 mol% Cu doped Ni electrode samples sintered at 1220 °C were prepared for TEM-EDX analysis, and the results are shown in Fig. 5. The TEM picture of the MLCC sample is shown in Fig. 5(a). Compared to the BCTZ phase (Fig. 5(b)), the metal phase has a high Ni signal intensity as well as a small Cu signal as shown in Fig. 5(c). The BCTZ phase has high signal intensity for Ba, Ca, Zr and Ti, with a small signal for Cu. It is therefore believed that the Cu2+ had diffused into BCTZ lattice.

A HRTEM micrograph and the electron diffraction patterns of BCTZ MLCC with Cu doped Ni electrode sintered at 1220 °C were obtained and are shown in Fig. 6; it can be seen that there is no intermetallic layers at the interface between BCTZ and metal electrode in the sample. This can be inferred from the homogeneous image contrast in the Ni grain up to the interface. This indicates that no severe reduction of BCTZ occurred in the samples. In contrast, a Ni(Ti, Ba) interfacial layer is always found in the commercial samples [10]. The Cu doped Ni electrodes were symbolized as **(A)**, and the BCTZ ceramics were symbolized as **(B)**. According to the electron diffraction patterns, the Cu doped Ni electrodes symbolized as **(A)** in Fig. 6(b) were constituted of a nickel phase. The BCTZ ceramic **(B)** was considered to be $BaTiO_3$ according to the electron diffraction patterns, as shown in Fig. 6(c).

3.3. *Effect of Cu doped Ni electrodes on the dielectric properties of BCTZ MLCC*

Fig. 7 shows the temperature coefficient of capacitance (TCC) as a function of the amount of Cu dopant in the nickel paste. For samples with of 0, 0.92, and 2.76 mol% Cu dopant, the Curie temperatures were 0 °C, 19.7 °C, and 14.3 °C, respectively. The Curie point shifted to a higher temperature with added Cu dopant. The dielectric constant and dielectric loss of the BCTZ ceramics as a function of the Cu dopants and sintering temperatures were determined at 1 kHz and the results are listed in Table 1. The ε_r value of the BCTZ MLCC without the addition of Cu sintered at 1220 °C was very low (~10,000) [24]. The dielectric constants of the BCTZ MLCC sintered at 1220 °C are 25216 and 24098 when doped with 0.92 mol% and 2.76 mol% Cu in Ni paste, respectively. It is clear that the dielectric constant of the BCTZ MLCC with Cu dopant sintered at 1220 °C is greater than without the Cu dopant, which can be attributed to the creation of lattice strain and good electrode continuity of the BCTZ MLCC with Cu doped Ni electrodes. The loss tangent of the 9

Table 1
The dielectric constant and dielectric loss of the BCTZ MLCCs as a function of the Cu dopants.

Cu (mol%)	Sintering temperature (°C)	Dielectric constant	Dielectric loss ($\times 10^{-4}$)	Insulation resistance (MΩ)	Curie point (°C)
0.92	1220	25,516	668	12,0433	19.7
2.76	1220	24,098	620	12,5937	14.3

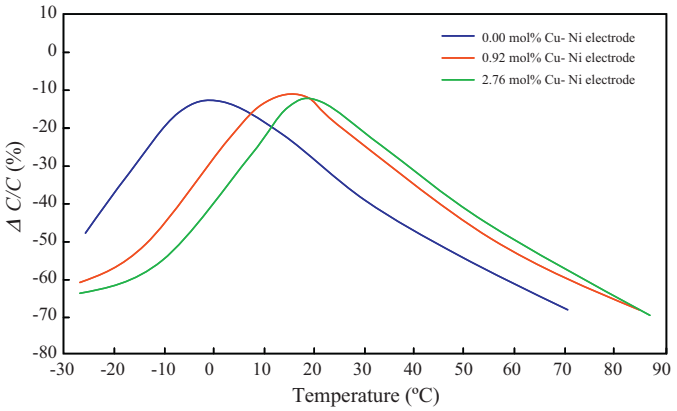

Fig. 7. Temperature coefficient of capacitance of BCTZ MLCC sintered at 1220 °C as a function of amount of added Cu in a Ni electrode. 14.

BCTZ MLCCs is also listed in Table 1. For samples with different Cu dopant ranging from 0.92 mol% to 2.76 mol%, the dielectric loss of BCTZ MLCCs is kept at same level. Additionally the insulation resistance of the samples with different sintering temperatures and Cu dopants are listed in Table 1. The insulation resistance of all samples were higher than 10^{11} Ω, implying the whole samples were well densification. Fig. 8 shows a plot of the insulation resistance versus inversed absolute temperature ($1/T$) for different Cu dopant amounts of BCTZ MLCCs sintered at 1220 °C. It can be seen that the IR of BCTZ MLCCs with a 0.92 mol% Cu doped Ni electrode decreases approximately linearly with inversed temperatures. However, the IR degradation with temperature is very severe for the samples with 2.76 mol% Cu doped Ni electrodes. The reason for this may be attributed to greater oxygen vacancies or a higher dislocation concentration in the BCTZ MLCCs with 2.76 mol% Cu doped Ni electrodes. As mentioned above, when Cu^{2+} substitutes into the B-site in the ABO_3 structure, a double ionized oxygen vacancy is formed. However, when an electric field is applied at high temperature, these ionized oxygen vacancies could give rise to leakage currents, so that the electrical IR of the specimens decreases. Rawal and Chan

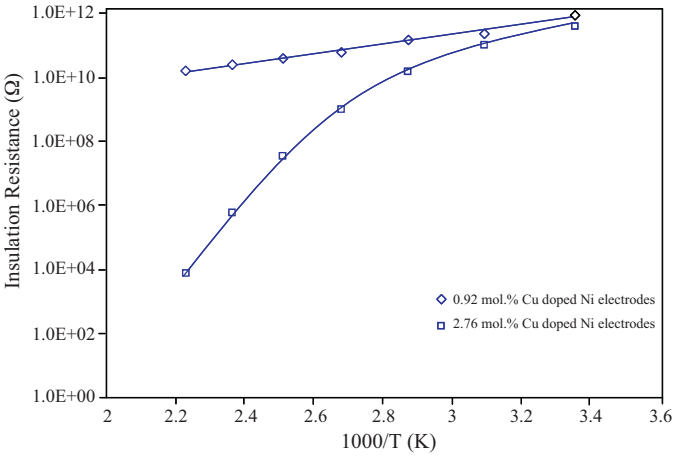

Fig. 8. Electrical resistances of the BCTZ MLCCs sintered at 1220 °C with different amount of Cu doped in Ni electrodes as a function of the reciprocal temperature.

[25] reported that IR degradation under a highly accelerated lift test may be classified into two modes, one is an avalanche breakdown (ABD), and the other one is a thermal runaway (TRA). ABD refers to the sudden breakdown accompanied by an abrupt leakage of current. TRA refers to the breakdown, which results from a gradual increase in the leakage current. Degradation modes may vary depending on the test conditions. ABD generally occurs when the test is accelerated by a voltage. Conversely, TRA generally occurs when the test is accelerated by temperature. Both ABD and TRA may be observed at the same time in some cases, depending on the test conditions. Imperfections in ceramics can be generally classified into two categories, intrinsic and extrinsic factors. Intrinsic factors are electronic disorders, dislocations, grain boundaries, defects, etc. Extrinsic factors are delamination, cracks, voids, pores, etc. ABD is said to 10 be caused by extrinsic factors and TRA to be caused by intrinsic factors [2]. Based on the above observations, it is believed that the dislocations and oxygen vacancies play an important role in dominating decrease in insulation resistance at high temperature life test.

4. Conclusions

The shrinkage behavior, microstructure development and dielectric properties of BCTZ MLCC with Cu doped Ni electrodes have been investigated. Good interfacial stability between BCTZ dielectric and Cu doped Ni electrode were obtained. The TEM conclusions revealed that there was almost no interaction between the Cu doped Ni electrodes and BCTZ dielectric layer. Unlike commercial MLCC, this result showed that the interface between Cu doped Ni electrodes and the BCTZ dielectric layer was very clean. The interface between BT dielectric and Ni electrode were observed in a commercial MLCC. In addition, BCTZ MLCC with a Cu doped Ni electrode has positive effects on the dielectric constant and electrode continuity, but the dielectric loss ($\tan\delta$) is slightly higher when compared to a standard MLCC.

References

[1] C.-L. Chen, W.-H. Lee, W.-C.J. Wei, Sintering behavior and interfacial analysis of Ni/Cu electrode with $BaTiO_3$ particulates, J. Electroceram. 14 (2005) 25–36.
[2] J. Yamamatsu, N. Kawano, T. Arashi, A. Sato, Y. Nakano, T. Nomura, Reliability of multilayer ceramic capacitors with nickel electrodes, J. Power Sources 60 (1996) 199–203.
[3] H. Saito, H. Chazono, H. Kishi, N. Yamaoka, The effect of rare-earth (La, Sm, Dy, Ho and Er) and Mg on the microstructure in $BaTiO_3$, Jpn. J. Appl. Phys. 30 (1991) 2307–2312.
[4] G. de With, Structural integrity of ceramic multilayer capacitor materials and ceramic multilayer capacitors, J. Eur. Ceram. Soc. 12 (11) (1993) 323–336.
[5] Y. Park, Y.H. Kim, H.G. Kim, The effect of grain size on dielectric behavior of $BaTiO_3$ based X7R materials, Mater. Lett. 28 (1996) 101–105.
[6] S. Sato, Y. Nakano, A. Sato, T. Nomura, Mechanism of improvement of resistance degradation in Y-doped $BaTiO_3$ based MLCCs with Ni electrodes under highly accelerated life testing, J. Eur. Ceram. Soc. 19 (1999) 1061–1067.
[7] A. Rae, M. Chu, V. Ganine, Barium titanate past, present and future, Ceram. Trans. "Dielectric Ceram. Mater." 100 (98) (1999) 1–12.
[8] T. Li, L.T. Li, Y. Kou, Z.L. Gui, Stable temperature dependenceof dielectric properties in $BaTiO_3$–Nb_2O_5–Co_3O_4–Gd_2O_3 system, J. Mater. Sci. Lett. 19 (11) (2000) 995–997.
[9] P. Hansen, D. Hennings, H. Schreinemacher, High-K dielectric ceramics from donor/acceptor-co-doped $(Ba_{1-x}Cax)(Ti_{1-y}Zry)O_3$ (BCTZ), J. Am. Ceram. Soc. 81 (5) (1998) 1369–1375.
[10] G.Y. Yang, S.I. Lee, Z.J. Liu, C.J. Anthony, E.C. Dickey, Z.K. Liu, C.A. Randall, Effect of local oxygen activity on Ni–$BaTiO_3$ interfacial reactions, Acta Mater. 54 (2006) 3513–3523.

[11] D.F.K. Hennings, Dielectric materials for sintering in reducing atmosphere, J. Eur. Ceram. Soc. 21 (2001) 1637–1642.
[12] S.K. Sarkar, M.L. Sharma, Liquid phase sintering of $BaTiO_3$ by boric oxide (B_2O_3) and lead borate (PbB_2O_4) glasses and its effect on dielectric strength and dielectric constant, Mater. Res. Bull. 15–24 (2) (2000) 407–416.
[13] M.A. Zubair, C. Leach, The influence of cooling rate and SiO_2 additions on the grain boundary structure of Mn-doped PTC thermistors, J. Eur. Ceram. Soc. 28 (2008) 1845–1855.
[14] N. Wang, M.-Y. Zhao, Z.-W. Yin, Low-temperature firing in microwave dielectric ceramic, J. Inorg. Mater. 17 (5) (2002) 915–924.
[15] S.P. Wu, Termination of BME-MLCC using copperenickel bimetallic powder as electrode material, IEEE Trans. Components Packaging Technol. 29 (4) (2006) 827e32.
[16] W. Songping, J. Li, N. Jing, Z. Zhenou, L. Song, Preparation of ultra fine copper-nickel bimetallic powders for conductive thick film, Intermetallics 15 (2007) 1316–1321.
[17] Y.-C. Wu, J.-S. Lee, H.-Y. Lu, C.-L. Hu, Microstructure analysis of the Y5V multilayer ceramic capacitors based on $BaTiO_3$, J. Electroceram. 18 (2007) 13–24.
[18] X.H. Wang, W.H. Lu, J. Liu, Y.L. Zhou, D.X. Zhou, Effects of La_2O_3 additions on properties of $Ba_{0.6}Sr_{0.4}TiO_3$–MgO ceramics for phase shifter applications, J. Eur. Ceram. Soc. 26 (2006) 1981–1985.
[19] H.T. Jiang, J.w. Zhai, X.j. Chou, X. Yao, Influence of Bi_2O_3 and CuO addition on low-temperature sintering and dielectric properties of $Ba_{0.6}Sr_{0.4}TiO_3$ ceramics, Mater. Res. Bull. 44 (2009) 566–570.
[20] C.L. Huang, W.R. Yang, Effect of CuO addition to $Nd(Zn_{1/2}Ti_{1/2})O_3$ ceramics on sintering behavior and microwave dielectric properties, Mater. Lett. 63 (1) (2009) 103–105.
[21] Y.C. Lee, W.H. Lee, F.S. Shieu, Microwave dielectric properties and microstructures of $Ba_2Ti_9O_{20}$-based ceramics with $3ZnO–B_2O_3$ addition, J. Eur. Ceram. Soc. 25 (2005) 3459–3468.
[22] F.A. Kroger, H.J. Vink, Relations between the concentrations of imperfections in crystalline solids, Solid State Phys. 3 (1956) 307–310.
[23] Y.-C. Lee, Y.-L. Huang, Effects of CuO doping on microstructural and dielectric properties of the $Ba_{0.6}Sr_{0.4}TiO_3$ ceramics, J. Am. Ceram. Soc. 92 (11) (2009) 2661–2667.
[24] Y.-C. Lee, C.-W. Lin, W.-J. Chen, W.-H. Lu, The Influence of SiO_2. Addition on the dielectric properties and microstructure of $(Ba_{0.96}Ca_{0.04})(Ti_{0.85}Zr_{0.15})O_3$. ceramics sintered in reducing atmosphere, Int. J. Appl. Ceram. Technol. 6 (6) (2009) 692–701.
[25] B.S. Rawal, N.H. Chan, Conduction and failure mechanisms in barium titanate based ceramics under highly accelerated conditions, AVXTech. Rep. (1984).